



## CP-Violation in Leptonic Sector

- CP-violation (CPV) responsible for matter/anti-matter asymmetry,  $A_{CP}$ :
  - It has been seen in the baryonic sector → not enough to explain the observed matter/anti-matter asymmetry<sup>1</sup>.
  - Not confirmed yet in the leptonic sector → T2K has reported closed 99.73% ( $3\sigma$ ) intervals on the CPV phase<sup>2</sup>.
- Neutrino mixing relates the neutrino flavor and mass eigenstates through the PMNS unitary matrix.

$$U = \begin{pmatrix} 1 & 0 & 0 \\ 0 & \cos\theta_{23} & \sin\theta_{23} \\ 0 & -\sin\theta_{23} & \cos\theta_{23} \end{pmatrix} \begin{pmatrix} \cos\theta_{13} & 0 & \sin\theta_{13}e^{-i\delta_{CP}} \\ 0 & 1 & 0 \\ -\sin\theta_{13}e^{i\delta_{CP}} & 0 & \cos\theta_{13} \end{pmatrix} \begin{pmatrix} \cos\theta_{12} & \sin\theta_{12} & 0 \\ -\sin\theta_{12} & \cos\theta_{12} & 0 \\ 0 & 0 & 1 \end{pmatrix}$$

Fig. 1: The PMNS matrix. The first matrix expresses the oscillation in the "23/atmospheric sector", the second matrix in the "13/reactor sector" and the third matrix in the "12/solar sector". The second matrix is responsible for the leptonic CP-violation.

## Project Objectives

- Aims at searching the CPV in the leptonic sector:
  - at  $5\sigma$  C.L. level (> 60% of the leptonic Dirac  $\delta_{CP}$ ).
  - precision measurement of  $\delta_{CP}$  value.
- Uses intense neutrino beam generated by the ESS 2.5 GeV, 5 MW LINAC proton beam in Lund (Sweden).
  - Measures at the 2<sup>nd</sup> oscillation maximum:
    - Advantage: ~ 3x higher in CPV sensitivity vs measuring at the 1<sup>st</sup> oscillation maximum.
    - The asymmetry,  $A_{CP}$ , at the 1<sup>st</sup> oscillation maximum is  $A_{CP} = 0.35 \sin(\delta_{CP})$  while at the 2<sup>nd</sup> is  $0.7 \sin(\delta_{CP})$ .



Fig. 2: Photo of the ESS site.

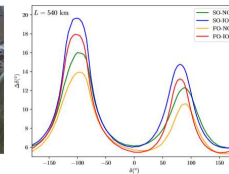


Fig. 3: Precision measurement for  $\delta_{CP}$ .

## Target-station facility

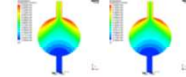
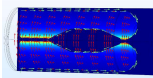
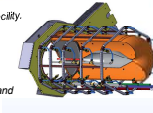
### 4Horn focusing system

- Four separated horns, target canister in the horn middle.
- Aluminum conductor with outer (10 mm)/inner (3 mm) thickness and water cooled.
- Horn current 350 kA/14 Hz/100  $\mu$ s-pulse.
- Toroidal  $\vec{B}$  field inside the cavity, with max. B-value of 2.21 T.
- Current polarity depends on the  $\pi^2$  focusing operation mode.
- has a very low inductance of 0.9  $\mu$ H and a low resistance value of 0.235 m $\Omega$ .



Fig. 4: Target-station facility.

Fig. 5: Target canister with cooling bars.



Cooling by transverse flow – temperature

Cooling by transverse flow – superficial velocity

### Packed-bed target

- Four solid packed-bed, 1.5 mm radius Ti spheres, contained in a 15 mm-radius, 780 mm-long canister.
- 1.25 MW @ of 14 Hz ESS proton beam on target.
- Cooled based on longitudinal He flow in the bulk of the canister
- Disadvantage: drastic reduction in cooling the spheres at the canister back.
- New multi-entries transverse cooling system is under study
- Advantage: homogenous cooling of the spheres in the canister bulk.

### Beam dump (Segmented-blocks core)

- Protects the site behind the decay tunnel from radio-activation.
- Different graphite core designs, with outer layout 4 x 4 x 3.2 m<sup>3</sup>.

Steady state analysis  
- Maximum Temp. = 522 K  
- Maximum von-Mises stress (thermal load only) = 207 MPa  
- Maximum displacement / structure-deformation = 1.46 mm.

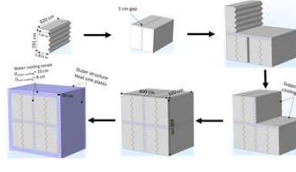


Fig. 7: Seg-blocks BD core assembly and thermo-structural performance.

## LINAC upgrade, accumulator ring and switchyard

- ESSνSB proposes to increase the ESS LINAC power from 5 MW to 10 MW.
- The dedicated proton beam will be shortened to 1.3  $\mu$ s:
  - with the help of the accumulator ring (in red).
  - will be split in four parts with a switchyard (yellow), before entering the target station.

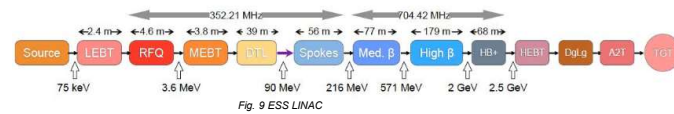


Fig. 9 ESS LINAC



Fig. 8: Layout of the ESS site.

- Due to the space charge formation, H<sup>-</sup> ions are injected into the LINAC and stripped by a foil before entering the accumulator.
- Ring-to-switchyard transfer-line extract the proton pulses from the ring to the beam switchyard and distribute the resulting four beam batches over four targets.

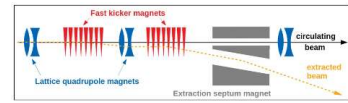


Fig. 10: Transfer-line (left) and switchyard (right).

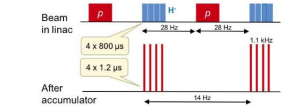
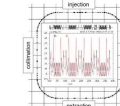


Fig. 11: Accumulator (left) and proton beam pulses (right).

- This solution fixes the technology chosen for the target producing the secondary particles.
- With 1.25 MW per target a packed bed target should work.

## Detectors and physics potential

### The near neutrino detector

- The Near Detector is based on the Water Cherenkov equipped with a Fine-grained Scintillator Tracker inside a magnetic field and an Emulsion neutrino detector for flux and cross sections measurements.

### The far neutrino detector

- Two water Cherenkov detectors with total fiducial mass of over 500 kt.
- 540 km-baseline/1.2 km-overburden.

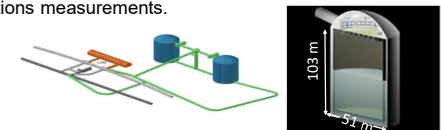
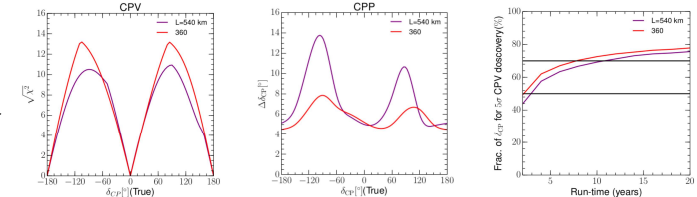


Fig. 12: Memphis-like far detector.

### Physics performance

- An optimized geometry of the Target Station and the improved efficiency in the event reconstruction at the FD, lead to an unprecedented precision which can be achieved in the measurement of the  $\delta_{CP}$  oscillation parameter<sup>3</sup>.
- Under a conservative estimate of the systematic errors signal/background of 5/10% , respectively, we observe:
  - More than  $12\sigma$  C.L. for  $\delta_{CP} = -90^\circ$  can be achieved for the location of the FD at 360 km (Zinkgruvan).
  - ~8° uncertainty on  $\delta_{CP}$  measurement for  $\delta_{CP} = -90^\circ$  for the same location.
  - More than 70% coverage of  $\delta_{CP}$  values covered at  $5\sigma$  in 10 years running time.

Fig. 13: (Left) significance of the CPV discovery. (Middle) Precision in the measurement of  $\delta_{CP}$ . (Right) Fraction of  $\delta_{CP}$  for 5 $\sigma$  CPV discovery.



- The upgrade of this facility can be used for other experiments and develop other techniques, e.g. muon cooling.